



HAL
open science

Electrical properties of highly disordered bismuth-based composites

F. Brochin, Bertrand Lenoir, C. Bellouard, H. Scherrer, I. Vurgaftman, J R Meyer

► **To cite this version:**

F. Brochin, Bertrand Lenoir, C. Bellouard, H. Scherrer, I. Vurgaftman, et al.. Electrical properties of highly disordered bismuth-based composites. *Physical Review B*, 2001, 63 (7), pp.073106. 10.1103/PhysRevB.63.073106 . hal-03996402

HAL Id: hal-03996402

<https://hal.science/hal-03996402>

Submitted on 19 Feb 2023

HAL is a multi-disciplinary open access archive for the deposit and dissemination of scientific research documents, whether they are published or not. The documents may come from teaching and research institutions in France or abroad, or from public or private research centers.

L'archive ouverte pluridisciplinaire **HAL**, est destinée au dépôt et à la diffusion de documents scientifiques de niveau recherche, publiés ou non, émanant des établissements d'enseignement et de recherche français ou étrangers, des laboratoires publics ou privés.

Electrical properties of highly disordered bismuth-based composites

F. Brochin, B. Lenoir, C. Bellouard, and H. Scherrer

Laboratoire de Physique des Matériaux, UMR No. 7556, Ecole des Mines, 54042 Nancy Cedex, France

I. Vurgaftman and J. R. Meyer

Code 5613, Naval Research Laboratory, Washington, D.C. 20375

(Received 5 September 2000; published 30 January 2001)

A pronounced classical size effect in the transport properties was observed in bulk bismuth-silica nanocomposites as a result of the limitation of the carrier mean free path by the grain size. From field- and temperature-dependent magnetotransport measurements, carrier mobility and density were explored in these highly disordered systems. The results clearly show modifications in the band parameters from those of bulk single-crystalline Bi.

DOI: 10.1103/PhysRevB.63.073106

PACS number(s): 72.80.Tm

Semimetallic bismuth, with a rhombohedral structure, exhibits many unique electrical transport properties. These derive from its highly anisotropic Fermi surface, low carrier density (five orders of magnitude lower than in ordinary metals), and very small electron effective mass along certain axes. Because of its large Fermi wavelength and long carrier mean free path (μ_n and μ_p , the electron and hole mobilities, can both exceed $10^6 \text{ cm}^2 \text{ V}^{-1} \text{ s}^{-1}$ at low temperatures¹), bismuth has been extensively investigated for quantum transport and both quantum and classical finite-size effects in low-dimensional systems.²⁻⁶

The combination of these unusual electrical properties with low thermal conductivity resulting from a heavy mass to scatter phonons enables bismuth to exhibit one of the highest thermoelectric figures of merit of any pure component. Theoretical works suggest that these thermoelectric properties could be improved by a random dispersion of particles of a few nanometers.^{7,8}

The production of nanocomposite ultrafine powders by simultaneous evaporation, nucleation, and growth is an attractive way to incorporate nanoinclusions into a material. Quite recently, we have developed an arc-plasma processing method for producing fine-grained polycrystalline bulk Bi containing SiO_2 nanoinclusions of variable concentration.^{9,10} It may ultimately be possible to reduce the thermal conductivity of such nanocomposite systems by a much greater degree than the electrical conductivity,¹¹ leading to enhanced thermoelectric figures of merit. Although the electronic properties of the highly disordered semimetallic Bi can be masked by prominent mixed conduction, the electron and hole transport may nonetheless be conveniently explored using the quantitative mobility spectrum analysis (QMSA) of magnetic-field-dependent Hall and resistivity data, whose effectiveness has already been highlighted in the case of Bi thin films.¹²

In this Brief Report, we present a magnetotransport investigation of bismuth-based nanocomposites. It will be seen from the extracted electron and hole densities and mobilities that an extrinsic behavior is clearly evidenced in these highly disordered materials at low temperatures. Employing the deduced band parameters, the thermoelectric power is calculated and compared to experimental results.¹⁰

The study was performed on one polycrystalline Bi sample and two Bi- SiO_2 nanocomposite samples containing 4 and 15 vol% of silica, respectively. The samples were prepared by consolidating powders produced by the arc-plasma technique. The preparation method and the microstructure of the powder are described in detail elsewhere.^{9,10} While the grain size for polycrystalline Bi is typically $1 \mu\text{m}$, the presence of silica inclusions in the nanocomposites inhibits the grain growth during sintering. The result is a grain size not exceeding 200 nm. X-ray diffraction indicated no preferential orientation of the grains. Magnetotransport measurements were carried out in ac at 40 Hz. A conventional four-probe technique was used for resistivity measurements, whereas a five-probe method was used for the Hall effect. The samples (typically $10 \times 2 \times 2 \text{ mm}^3$) were connected to Cu wires using low-temperature solder. The measurements were done in a variable-temperature cryostat mounted in a superconducting coil which provided magnetic fields up to $\pm 7 \text{ T}$ at temperatures spanning the range 4.2–300 K.

Figure 1 shows temperature-dependent electrical resistivities for all three samples. Values averaged over the crystal axes for a Bi single crystal¹³ are also given for comparison

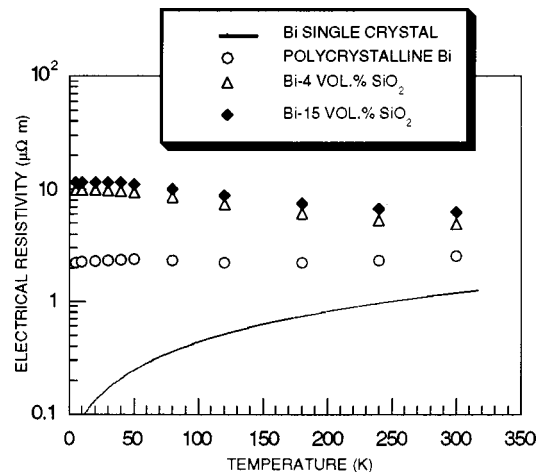


FIG. 1. Temperature-dependent electrical resistivities of the polycrystalline Bi and Bi- SiO_2 samples. The solid curve represents the averaged value for a Bi single crystal (Ref. 13).

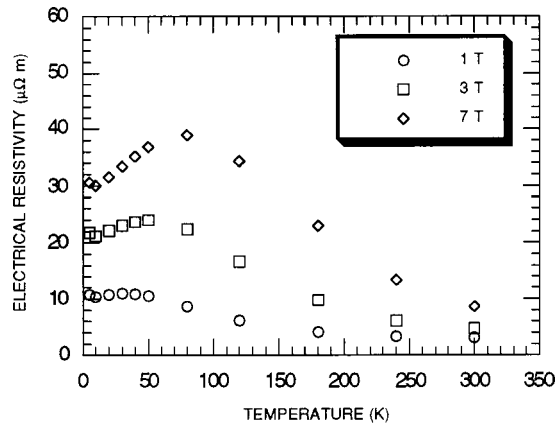


FIG. 2. Temperature dependence of the resistivity for the polycrystalline Bi at three magnetic fields.

(solid curve). The electrical resistivities for the Bi polycrystalline samples are quite constant ($\sim 2 \mu\Omega \text{ m}$), and higher than the average value for the single crystal at all temperatures. The resistivities of the nanocomposites increase with decreasing temperature until 30 K, below which they are nearly constant. Note that a negative temperature coefficient of resistivity (TCR) is usually observed for Bi thin films and Bi nanowires,^{3,5} while the TCR is positive for bulk single-crystal Bi.¹³ For both polycrystalline and single-crystal Bi, the temperature dependence of the resistivity represents a competition between the strong increase in the intrinsic carrier density with T and the strong decrease in the carrier mobility. The mobility dominates in the single crystal, resulting in a positive TCR. In the polycrystal at low temperature, however, the mean free path, which can reach the millimeter scale in perfect material,¹⁴ becomes limited by the grain boundaries. Hence, either a positive or a negative TCR is possible, depending on the grain size. Since there is more grain-boundary scattering in the materials with the smallest grain size (200 nm in the nanocomposite), the effect is more pronounced. The influence of the silica volume fraction on the resistivity is to shift the curve to higher values, as predicted by theory.⁸

The application of a magnetic field increases the sample resistivity, as illustrated in Fig. 2 for the case of the polycrystalline Bi. Note also that the temperature dependence of the resistivity acquires a distinct maximum at higher fields, which is related to the large positive magnetoresistance induced by mixed conduction and anisotropy. The temperature of the magnetoresistance peak is determined by a trade-off of the maximum mobility-field product (μB) at lower temperatures with greater mixed conduction at higher temperatures (see below). For the case of polycrystalline Bi with an applied magnetic field of 7 T, the magnetoresistance is about 250% at room temperature and increases to about 1600% at 80 K. Reducing the grain size from 1 to 0.2 μm decreases the magnetoresistance as a result of a shorter carrier mean free path (lower mobility).

To further our understanding of the electronic properties of these highly disordered materials, we have used the QMSA technique,^{15,16} which accounts for the anisotropy of the carrier mobilities,¹⁷ to determine the electron and hole

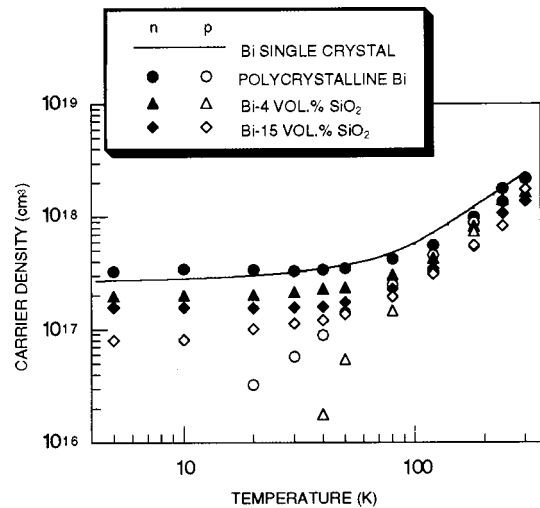


FIG. 3. Experimental (QMSA procedure) results for the electron and hole densities as a function of temperature for the polycrystalline Bi and Bi-4 vol % SiO_2 and Bi-15 vol % SiO_2 nanocomposites. The line represents the carrier density for a Bi single crystal (data extrapolated between 15 and 80 K) from Refs. 1 and 18.

densities and mobilities from the experimental variations of the resistivities and Hall coefficients with magnetic field. Resulting electron and hole concentrations as a function of temperature are given in Fig. 3 for the polycrystalline Bi and two nanocomposite samples. For comparison, the curve also shows the typical dependence from the literature for undoped single-crystal bulk Bi with overlapping conduction and valence bands and $n=p$.^{1,18} Note, however, that extrinsic behavior ($n > p$) is observed in the present polycrystalline samples at low temperatures. The samples have a net n -type carrier concentration of about $(2-3) \times 10^{17} \text{ cm}^{-3}$, although a smaller hole concentration is also present at all T in the sample with 15% SiO_2 nanoinclusions. With increasing temperature, the n/p ratio decreases and approaches unity to within experimental uncertainty at 300 K. The 300 K densities $n \sim p \sim 2 \times 10^{18} \text{ cm}^{-3}$ in the polycrystalline materials are close to the bulk Bi results of Michenaud and Issi.¹⁸

Previous studies of Bi thin films have found both n -type² and p -type¹² net carrier concentrations to be present at low temperatures. This extrinsic behavior has been attributed to the presence of defect states at the free surface of the thin films or at the interface with the substrate. In the case of our polycrystalline bulk materials, the extrinsic carriers could result either from surface states induced by the grain boundaries (point or line defects, dangling bonds, etc.) or from extrinsic defects (e.g., segregation, impurities). It is perhaps surprising that the measured net doping levels were actually slightly lower in the two nanocomposite samples, which have smaller grains. In fact, both n and p are suppressed in the low-temperature limit (in one case no holes are detectable). The effect appears to exceed the experimental uncertainty, although at this point one cannot strictly rule out its being a measurement artifact. If genuine, the finding implies a slightly smaller overlap of the electron and hole energy bands in the nanocomposite samples. Although the grains are too large (0.2 μm) for quantum size effects to significantly

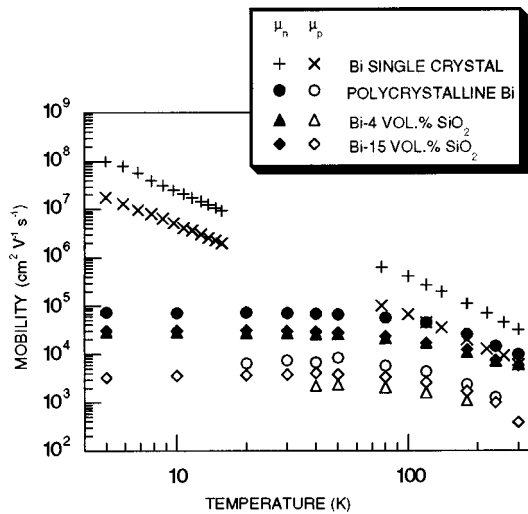


FIG. 4. Experimental (QMSA procedure) electron and hole mobilities as a function of temperature for the polycrystalline Bi, and the Bi-4 vol % SiO₂ and Bi-15 vol % SiO₂ nanocomposites. Also shown are reported mobilities for Bi single crystals (Refs. 1 and 18).

reduce the overlap, strain may be playing a role.

Figure 4 illustrates experimental mobilities for electrons (μ_n) and holes (μ_p) in the three samples. For comparison, the graph also includes data from the literature for μ_n and μ_p in Bi single crystals.^{1,18} The mobilities for both carriers are suppressed at low temperature due to grain-boundary scattering, as expected, whereas at high temperatures the electron mobility approaches the single-crystal value. The apparent observation of high- T hole mobilities somewhat below the single-crystal values may be artificial, since there is reduced sensitivity to the lower-mobility carrier properties in that regime where $\mu_p B \ll 1$. However, the finding of a higher mobility ratio μ_n/μ_p even at low T is probably a real consequence of the dominance by boundary scattering (rather than phonon scattering) in the present disordered material system.

The thermoelectric power (TEP) was calculated, accounting for the full anisotropic and nonparabolic band structure with literature values for the effective-mass parameters.¹⁹ The band overlap was adjusted downward by 15–20 meV from its bulk value of 38 meV in order to fit the QMSA carrier densities. Boundary roughness scattering was assumed to limit the low-temperature mobility (electron and hole scattering times of 0.12 and 1.2 ps were calculated for the polycrystalline Bi), and at higher temperatures the com-

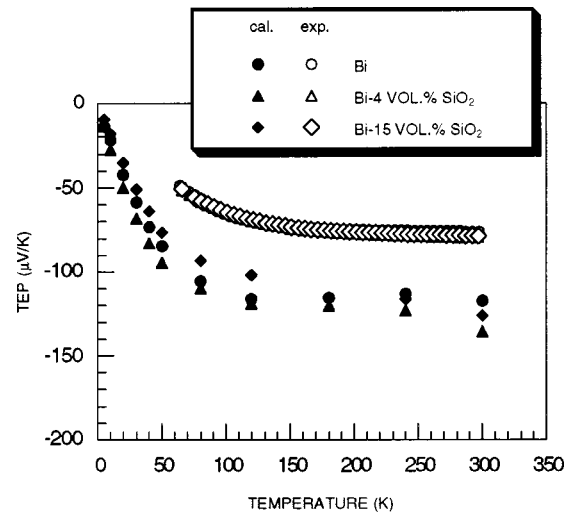


FIG. 5. Comparison between the experimental (Ref. 10) and calculated values of the TEP for polycrystalline Bi and Bi-4 vol % SiO₂ and Bi-15 vol % SiO₂ nanocomposites.

bined contribution of intravalley and electron-hole interband acoustic phonon scattering²⁰ was derived from the temperature variation of the mobilities. Whereas the QMSA hole mobilities were used at low temperatures, at higher T where the magnetotransport data were insensitive to p the hole mobility was assumed to be a factor of 2.7 lower than the electron mobility in agreement with literature values.¹⁹ The resulting theoretical TEP's are compared to the measurements in Fig. 5. Although theory overestimates the experimental values somewhat, the qualitative agreement is quite reasonable. The remaining discrepancy could be ascribed to analysis uncertainties and the difficulty of separating the intravalley and interband acoustic phonon mechanisms with different energy dependences of the momentum relaxation time.

In summary, we have clearly observed finite-size effects on the transport properties of polycrystalline Bi with different grain sizes. Field- and temperature-dependent magnetotransport have been analyzed by mixed-conduction techniques. With this approach, the band parameters were extracted. It was shown that grain-boundary scattering affects the band parameters and causes characteristic deviations from the bulk single-crystal behavior.

We thank LakeShore Cryotronics, Inc. for use of the quantitative mobility spectrum analysis algorithm.

¹R. Hartman, Phys. Rev. **181**, 585 (1979).

²Yu. F. Komnik, E. I. Bukhshtab, Yu. V. Nikitin, and V. V. Andrievskii, Zh. Eksp. Teor. Fiz. **60**, 669 (1971) [Sov. Phys. JETP **33**, 364 (1971)].

³N. Garcia, Y. H. Kao, and M. Strongin, Phys. Rev. B **5**, 2029 (1972).

⁴V. Damodara Das and N. Soundarajan, Phys. Rev. B **35**, 5990 (1987).

⁵K. Liu, C. L. Chien, and P. C. Searson, Phys. Rev. B **58**, 14 681 (1998).

⁶K. Liu, C. L. Chien, P. C. Searson, and K. Y. Zhang, Appl. Phys. Lett. **73**, 1436 (1998).

⁷G. A. Slack and M. A. Hussain, J. Appl. Phys. **70**, 2694 (1991).

⁸D. P. White and P. G. Klemens, J. Appl. Phys. **71**, 4258 (1992).

⁹F. Brochin, X. Devaux, J. Ghanbaja, and H. Scherrer, Nanostruct. Mater. **11**, 1 (1999).

- ¹⁰F. Brochin, B. Lenoir, X. Devaux, R. Martin-Lopez, and H. Scherrer, *J. Appl. Phys.* **88**, 3269 (2000).
- ¹¹N. Scoville, C. Bajgar, J. Rolfe, J. P. Fleurial, and J. Vandersande, *Nanostruct. Mater.* **5**, 207 (1995).
- ¹²C. A. Hoffman, J. R. Meyer, F. J. Bartoli, A. DiVenere, X. J. Yi, C. L. Hou, H. C. Wang, J. B. Ketterson, and G. K. Wong, *Phys. Rev. B* **48**, 11 431 (1993).
- ¹³J.-P. Issi, *Aust. J. Phys.* **32**, 585 (1979).
- ¹⁴D. H. Reneker, *Phys. Rev. Lett.* **1**, 440 (1958).
- ¹⁵J. R. Meyer, C. A. Hoffman, F. J. Bartoli, D. A. Arnold, S. Sivananthan, and J. P. Faurie, *Semicond. Sci. Technol.* **8**, 805 (1993).
- ¹⁶I. Vurgaftman, J. R. Meyer, C. A. Hoffman, D. Redfern, J. Antoszewski, F. Faraone, and J. R. Lindemuth, *J. Appl. Phys.* **84**, 4966 (1998).
- ¹⁷I. Vurgaftman, J. R. Meyer, C. A. Hoffman, S. Cho, J. B. Ketterson, F. Faraone, J. Antoszewski, and J. R. Lindemuth, *J. Electron. Mater.* **28**, 548 (1999).
- ¹⁸J.-P. Michenaud and J.-P. Issi, *J. Phys. C* **5**, 3061 (1972).
- ¹⁹I. Vurgaftman, J. R. Meyer, C. A. Hoffman, S. Cho, A. DiVenere, G. K. Wong, and J. B. Ketterson, *J. Phys.: Condens. Matter* **11**, 5157 (1999).
- ²⁰Yu. I. Ravich and A. V. Rapoport, *Fiz. Tverd. Tela (Leningrad)* **34**, 1801 (1992) [*Sov. Phys. Solid State* **34**, 960 (1992)].